Ab initio study of the thermopower of biphenyl-based single-molecule junctions

M. Bürkle,[1,2,*] L. A. Zotti,[3] J. K. Viljas,[4,5] D. Vonlanthen,[6] A. Mishchenko,[7] T. Wandlowski,[7] M. Mayor,[2,6,8] G. Schön,[1,2,8] and F. Pauly[1,2,9]

[1]*Institute of Theoretical Solid State Physics, Karlsruhe Institute of Technology, D-76131 Karlsruhe, Germany*
[2]*DFG Center for Functional Nanostructures, Karlsruhe Institute of Technology, D-76131 Karlsruhe, Germany*
[3]*Departamento de Física Teórica de la Materia Condensada, Universidad Autónoma de Madrid, E-28049 Madrid, Spain*
[4]*Low Temperature Laboratory, Aalto University, P.O. Box 15100, FIN-00076 Aalto, Finland*
[5]*Department of Physics, P.O. Box 3000, FIN-90014 University of Oulu, Finland*
[6]*Department of Chemistry, University of Basel, CH-4056 Basel, Switzerland*
[7]*Department of Chemistry and Biochemistry, University of Bern, CH-3012 Bern, Switzerland*
[8]*Institute for Nanotechnology, Karlsruhe Institute of Technology, D-76344 Eggenstein-Leopoldshafen, Germany*
[9]*Molecular Foundry, Lawrence Berkeley National Laboratory, Berkeley, California 94720, USA*

(Received 25 February 2012; revised manuscript received 9 July 2012; published 4 September 2012)

By employing *ab initio* electronic-structure calculations combined with the nonequilibrium Green's function technique, we study the dependence of the thermopower Q on the conformation in biphenyl-based single-molecule junctions. For the series of experimentally available biphenyl molecules, alkyl side chains allow us to gradually adjust the torsion angle φ between the two phenyl rings from 0° to 90° and to control in this way the degree of π-electron conjugation. Studying different anchoring groups and binding positions, our theory predicts that the absolute values of the thermopower decrease slightly towards larger torsion angles, following an $a + b\cos^2\varphi$ dependence. The anchoring group determines the sign of Q and a,b simultaneously. Sulfur and amine groups give rise to $Q,a,b > 0$, while for cyano, $Q,a,b < 0$. The different binding positions can lead to substantial variations of the thermopower mostly due to changes in the alignment of the frontier molecular orbital levels and the Fermi energy. We explain our *ab initio* results in terms of a π-orbital tight-binding model and a minimal two-level model, which describes the pair of hybridizing frontier orbital states on the two phenyl rings. The variations of the thermopower with φ seem to be within experimental resolution.

DOI: 10.1103/PhysRevB.86.115304 PACS number(s): 73.63.Rt, 85.65.+h, 85.80.Fi, 81.07.Pr

I. INTRODUCTION

Tailored nanostructures hold promise for improved efficiencies of thermoelectric materials.[1–3] For this reason, there is a growing interest to gain a better understanding of the role of interfaces on thermoelectric properties at the atomic scale. Controlled metal-organic interfaces can be studied using single-molecule junctions, and recently the thermopower of these systems was determined in first experiments.[4] While the thermopower (or Seebeck coefficient) of metallic atomic contacts was measured already several years ago,[5] molecular junctions offer fascinating possibilities to adjust thermoelectric properties due to the control over chemical synthesis and interface structure. Reference 4 and subsequent experimental studies thus explored the influence of different parameters on the thermopower, such as molecule length,[4,6,7] substituents,[8] anchoring groups,[7–9] or electrode metal.[10]

On the theory side, the electronic contribution to the thermopower explains important experimental observations.[11] We have shown recently that the thermopower of metallic atomic contacts, which serve as reference systems in molecular electronics, can be understood by considering the electronic structure of disordered junction geometries.[12] Using molecular dynamics simulations of many junction stretching processes combined with tight-binding-based electronic-structure and transport calculations, we found thermopower-conductance scatter plots similar to the low-temperature experiment.[5] Such a statistical analysis, although highly desirable for molecular junctions, is complicated by the time-consuming electronic-structure calculations needed to describe these heteroatomic systems. Still, early studies of the thermopower based on density functional theory (DFT) for selected geometries explained crucial trends, such as the dependence of the thermopower on molecule length[13] or the influence of substituents and anchoring groups.[13,14] Since the experiments on the thermopower of molecular junctions were all performed at room temperature until now, finite-temperature effects may play a role. They can impact the thermopower by fluctuations of the junction geometry and electron-vibration couplings.[12,15,16] While their quantification constitutes an interesting challenge for future work, we will focus here on the purely electronic effects in static ground-state contact structures.

An interesting aspect, not yet addressed in the experiments, is the influence of conjugation on the thermopower Q. For the conductance, such studies were carried out by different groups with biphenyl molecules.[17–19] The torsion angle φ between the phenyl rings was adjusted stepwise by use of appropriate side groups. While such substituents may have a parasitic shifting effect on energies of current-carrying molecular orbitals, the changes in conformation, which control the degree of π-electron conjugation, turned out to dominate the behavior of the conductance.[17] The systematic series of biphenyl molecules of Refs. 18–21 uses alkyl chains of various lengths and methyl groups to adjust φ and avoids strongly electron-donating and electron-withdrawing substituents. Hence, it seems ideal for determining the influence of conjugation on thermopower.

Theoretical work has considered the behavior of Q when φ is changed continuously for the thiolated biphenyl molecule

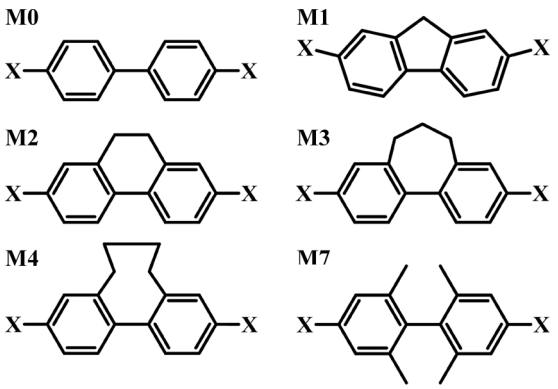

FIG. 1. Chemical structure of the studied biphenyl molecules with X standing either for the S, NH_2, or CN anchoring group.

contacted to gold (Au) electrodes.[13,22] Both studies agree on the fact that Q is positive for all φ. However, while we predicted Q to decrease with increasing φ based on DFT calculations and a π-orbital tight-binding model (TBM),[13] work of Finch *et al.*[22] suggested the opposite for this idealized system. In this study, we clarify this contradiction and demonstrate with the help of a two-level model (2LM) that for the off-resonant transport situation, the absolute value of Q is expected to decrease when the molecule changes from planar to perpendicular ring orientation. This confirms our previous conclusions. More importantly, this work explores the possibility to measure the dependence of Q on φ for the experimentally relevant family of molecules presented in Refs. 18–21.

Using DFT calculations of the electronic structure combined with the Landauer-Büttiker scattering formalism expressed with Green's function techniques, we determine the thermopower of biphenyl-derived molecules connected to gold electrodes. The molecules investigated are displayed in Fig. 1. Alkyl chains, one to four CH_2 units long, allow us to change φ gradually from 0° to 60°. To achieve $\varphi \approx 90°$, we included in addition M7, and as a reference also M0, the "standard" biphenyl molecule. For each of the molecules in Fig. 1, we explore the three different anchoring groups sulfur (S), amine (NH_2), and cyano (CN) in various binding geometries.

This work is organized as follows. In Sec. II, we introduce the theoretical procedures used in this work. Section III presents the main results. We start by discussing models to describe the φ dependence of the thermopower, show the DFT-based results for Q, and provide further insights by discussing their relation to the predictions of the TBM and the 2LM. The paper ends with the conclusions in Sec. IV.

II. THEORETICAL METHODS

A. Electronic structure and contact geometries

We determine the electronic structure and contact geometries in the framework of DFT. All our calculations are performed with the quantum chemistry package TURBOMOLE 6.3,[23] and we use the gradient-corrected BP86 exchange-correlation functional.[24,25] For the basis set, we employ def2-SV(P) which is of split-valence quality with polarization functions on all nonhydrogen atoms.[26] For Au, an effective core potential efficiently deals with the innermost 60 electrons,[27] while the basis set provides an all-electron description for the rest of the atoms in this work.

The contact geometries for the S-terminated molecules are those of Ref. 28. For the NH_2 and CN anchors, we proceed as described in Refs. 19 and 28 and use for consistency the electrode geometry from Ref. 28.

B. Charge transport

We determine charge-transport properties in the phase-coherent limit using the Landauer-Büttiker formalism. The transmission function $\tau(E)$, describing the energy-dependent transmission probability of electrons through the nanostructure, is calculated with Green's function techniques. The Green's functions are constructed by use of the DFT electronic structure as obtained for the ground-state molecular junction geometries. A detailed description of our quantum transport method is given in Ref. 29.

The thermopower at the average temperature T is defined as the ratio of the induced voltage difference ΔV in the steady state and the applied temperature difference ΔT between the ends of a sample, $Q(T) = -(\Delta V/\Delta T)|_{I=0}$. Using the Landauer-Büttiker formalism, the electronic contribution to the thermopower in the linear response regime can be expressed as[30]

$$Q(T) = -\frac{K_1(T)}{eTK_0(T)} \tag{1}$$

with $K_n(T) = \int dE\tau(E)(E-\mu)^n[-\partial f(E,T)/\partial E]$, the absolute value of the electron charge $e = |e|$, the Fermi function $f(E,T) = \{\exp[(E-\mu)/k_BT]+1\}^{-1}$, the Boltzmann constant k_B, and the chemical potential $\mu \approx E_F = -5$ eV, which approximately equals the Fermi energy E_F of the Au electrodes. The nonequilibrium situation beyond linear response can be described following Refs. 15, 31, and 32, but is not studied here. At low temperatures, performing a Sommerfeld expansion, Eq. (1) simplifies to[11,30]

$$Q(T) = -q(T)\frac{\partial_E\tau(E)}{\tau(E)}\bigg|_{E_F} \tag{2}$$

with the prefactor $q(T) = \pi^2k_B^2T/(3e)$ depending linearly on temperature.

While the measurements of the thermopower of metallic atomic contacts were performed at a low temperature of $T = 12$ K,[5] the experiments for molecular contacts were, until now, carried out at room temperature.[4,6–10] Finite temperatures impact the thermopower by the broadening of the Fermi distribution in the electrodes, as described by Eqs. (1) and (2). Additional effects result from thermal fluctuations of the junction geometry or the coupling of charge carriers and vibrations. The geometrical fluctuations can be taken into account by a thermal average over different junction geometries or finite-temperature molecular dynamics simulations.[12,16,33] The electron-phonon coupling and related inelastic effects can modify the thermopower in a more intricate way,[15] leading for instance to phonon drag.[34]

To avoid these complications and justify the use of static junction geometries and Green's functions derived from the ground-state electronic structure, we calculate in the following the thermopower for a low temperature of $T = 10$ K, if not

otherwise indicated. For the DFT-based results presented in the following, we determine Q by means of Eq. (1), i.e., by taking into account the full energy dependence of the transmission function. For the molecular junctions studied here, the differences to the values obtained via Eq. (2) often turn out to be small even at room temperature ($T = 300$ K) due to the smooth transmissions $\tau(E)$ around E_F. Hence, thermopower values for higher T can be estimated using the values at 10 K through $Q(T) \approx (T/10\,\mathrm{K}) \times Q(10\,\mathrm{K})$. Since we are not primarily interested in the temperature dependence of Q in this work, we suppress from here on the temperature argument.

III. RESULTS AND DISCUSSION

A. Models for the angle-dependent thermopower

In Ref. 13, we argued that the thermopower should depend on the torsion angle as

$$Q_\varphi \approx a + b\cos^2\varphi. \tag{3}$$

Our argument was based on the observation that for a π-orbital TBM in the off-resonant transport situation, the transmission of the biphenyl molecule can be expanded in powers of $\cos^2\varphi$ as[13,33,35]

$$\tau_\varphi(E) = \alpha_2(E)\cos^2\varphi + \alpha_4(E)\cos^4\varphi + O(\cos^6\varphi). \tag{4}$$

Conductance measurements[17–19] and corresponding DFT calculations,[33] which both determine the transmission at the Fermi energy, show that α_2 is the dominant term. The leading term in the φ dependence of Q is obtained from Eq. (2) by taking into account the energy dependence of the expansion coefficients $\alpha_j(E)$ and considering the terms up to $j = 4$. Then, we obtain Eq. (3) with

$$a = -q\frac{\partial_E\alpha_2(E)}{\alpha_2(E)}\bigg|_{E=E_F}, \tag{5}$$

$$b = -q\frac{\alpha_2(E)\partial_E\alpha_4(E) - \alpha_4(E)\partial_E\alpha_2(E)}{\alpha_2(E)^2}\bigg|_{E=E_F}. \tag{6}$$

While this model uses minimal information about the biphenyl molecular junction, a disadvantage is that the magnitude and energy dependence of the coefficients α_2 and α_4 are *a priori* unknown.

An alternative strategy is to use the 2LM of Ref. 18. This minimal model explains the $\cos^2\varphi$ law of the conductance by considering the pair of hybridizing frontier orbital resonances of the phenyl rings which are closest to E_F. Within this model, the transmission is given by[18]

$$\tau_\varphi(E) = \left|\frac{\tilde\Gamma\tilde t'(\varphi)}{[E-\tilde\varepsilon_s(\varphi)-i\tilde\Gamma/2][E-\tilde\varepsilon_a(\varphi)-i\tilde\Gamma/2]}\right|^2 \tag{7}$$

with $\tilde\varepsilon_{s,a}(\varphi) = \tilde\varepsilon_0 \pm \tilde t'(\varphi)$. Here, $\tilde\varepsilon_0$ describes the relevant frontier molecular orbital energy of the individual phenyl ring. For the biphenyl molecule, it can be determined as the doubly degenerate highest occupied molecular orbital (HOMO) or lowest unoccupied molecular orbital (LUMO) energy at $\varphi = 90^\circ$. The angle-dependent inter-ring coupling $\tilde t'(\varphi) \approx \tilde t\cos\varphi$ leads to a splitting of the pair of degenerate levels $\tilde\varepsilon_0$ at energies $\tilde\varepsilon_{s,a}(\varphi)$ with symmetric and antisymmetric wave functions, respectively. In addition, we have made the wide-band approximation with a symmetric and energy-independent coupling $\tilde\Gamma$ to the left and right phenyl rings. The 2LM is hence characterized by the parameters $\tilde\varepsilon_0, \tilde t, \tilde\Gamma$.

We set $\tilde\varepsilon = \tilde\varepsilon_0 - E_F$, $\tilde x = \tilde t\cos\varphi/\sqrt{\tilde\varepsilon^2 + \tilde\Gamma^2/4}$, and assume $|\tilde x| \ll 1$. Performing a Taylor expansion in $\tilde x$, we obtain Eq. (3) with

$$a = -q\frac{4\tilde\varepsilon}{\tilde\varepsilon^2 + \tilde\Gamma^2/4}, \tag{8}$$

$$b = -q\frac{4\tilde t^2\tilde\varepsilon(\tilde\varepsilon^2 - 3\tilde\Gamma^2/4)}{(\tilde\varepsilon^2 + \tilde\Gamma^2/4)^3}. \tag{9}$$

These expressions predict that the sign of a, b is determined by $\tilde\varepsilon$. Thus, when $\tilde\varepsilon$ changes sign, a, b change sign at the same time. In the typical off-resonant transport situation $|\tilde\varepsilon| \gg |\tilde t|, \tilde\Gamma$, the sign of $a \approx -q4/\tilde\varepsilon$ and $b \approx -q4\tilde t^2/\tilde\varepsilon^3$ is identical. However, b may be of a different sign than a in a more on-resonant case when the broadening $\tilde\Gamma$ is of a similar size as $\tilde\varepsilon$, i.e., when $\tilde\varepsilon^2 - 3\tilde\Gamma^2/4$ changes sign.

B. Thermopower based on density functional theory

For each of the biphenyl molecules in Fig. 1, we study the three different anchoring groups $X = \mathrm{S}, \mathrm{NH_2}, \mathrm{CN}$ and select a total of seven contact geometries, as displayed in Fig. 2. For S anchors, we choose three representative binding sites,[28,36] where S binds covalently either to three Au atoms in the hollow position (S-HH), to two of them in the bridge position (S-BB), or to a single one in the top position (S-TT1). NH_2- and CN-terminated molecules bind selectively to a single Au electrode atom at each side via the nitrogen lone pair.[19,37] Thus, we consider two different top sites for NH_2 (NH_2-TT1, NH_2-TT2) and CN (CN-TT1, CN-TT2), respectively.

In Table I, we summarize the torsion angle φ, which is defined as the dihedral angle between the two phenyl rings (see Fig. 3), and the thermopower for all 42 molecular junctions studied. The data are presented graphically in Fig. 3 by plotting Q as a function of φ for each of the seven types of junctions in Fig. 2. We notice that the sign of the thermopower is determined by the anchoring group. For the electron-donating S and NH_2 linkers,[38] the energy of the π-electron system of the molecules is increased compared to the hydrogen-terminated case ($X = \mathrm{H}$ in Fig. 1). The HOMO energy is therefore close to E_F, as visible also from the transmission curves in Fig. 4. The hole conduction through the HOMO yields $Q > 0$, in agreement with previous experimental[4,6] and theoretical results.[13,14] In contrast to this, for the electron-withdrawing CN anchoring group,[38] we have electron transport through the LUMO (Refs. 8, 14, 19, and 39; see also Fig. 4), and consequently $Q < 0$.

Considering the absolute values of the thermopower, Fig. 3 shows that Q can differ markedly for the types of contact geometries. Given the off-resonant transport situation suggested by the transmission curves in Fig. 4 and using Eqs. (8) and (9), we can understand the results by changes in the level alignment $\tilde\varepsilon$. As we will discuss in more detail in Sec. III C, level broadenings $\tilde\Gamma$ and couplings $\tilde t$ play no important role in that respect. The level alignment is determined by the charge transfer between the molecule and the electrodes, which is sensitive to the binding site of the anchoring group at the

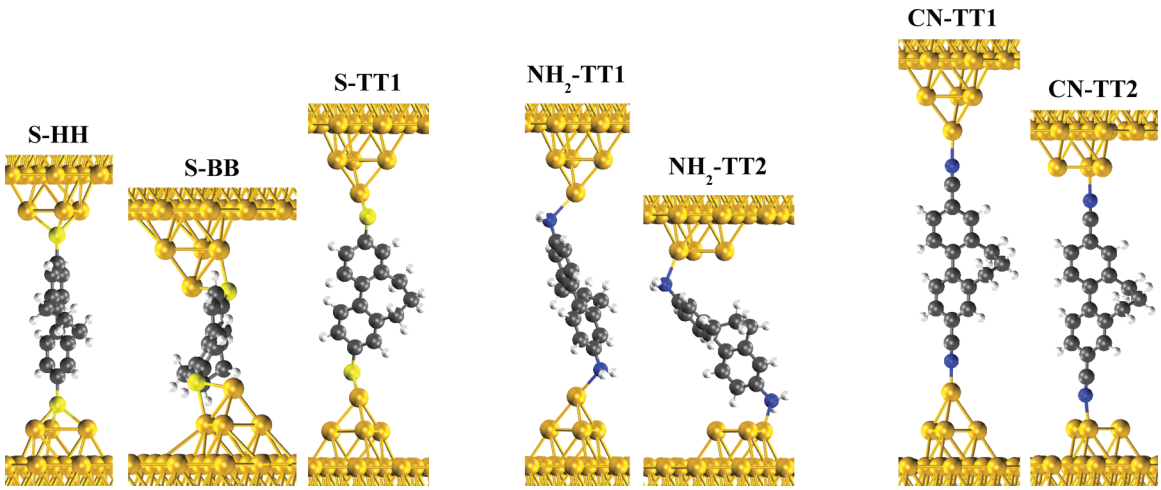

FIG. 2. (Color online) Analyzed types of junctions, shown for M3. For S anchors we consider hollow, bridge, and top binding sites to Au with the corresponding contact geometries called S-HH, S-BB, and S-TT1, respectively. For NH_2 and CN, we consider binding to single Au atoms in two different top positions with the contacts named NH_2-TT1, NH_2-TT2 and CN-TT1, CN-TT2.

molecule-metal interface. For the thiolated molecules, we find that the thermopower for S-BB and S-TT1 is comparable, but the values are significantly larger than those for S-HH. This behavior is related to our recent findings for the conductance of the thiolated molecules, where top and bridge geometries yield similar but much larger conductances than those with hollow sites.[28] Both observations are due to a HOMO level which is more distant from E_F for S-HH as compared to S-BB and S-TT1. We explain this by the leakage of electrons from the molecule, including the S atoms, to the Au electrodes, when going from the S-TT1 over the S-BB to the S-HH geometry.[28] For the amines, NH_2-TT1 gives a larger thermopower than NH_2-TT2. We have checked that this is a result of the larger negative charge on the molecule when bonded in NH_2-TT1 position as compared to NH_2-TT2, which moves the HOMO closer to E_F. With respect to the thiols, we see that both NH_2-linked geometries give rise to a thermopower well below those of S-BB and S-TT1 but still larger than for S-HH. The CN-linked molecules show the largest $|Q|$. The more positive charge on the molecules in CN-TT1 as compared to CN-TT2 leads to their smaller, i.e., more negative Q.

Regarding M0 with $X = \mathrm{S}, \mathrm{NH_2}$, we can compare to experimental and theoretical results for Q in the literature. For biphenyl-diamine, a thermopower of $Q_{\mathrm{M0}}^{\mathrm{NH_2-EXPT}} = 4.9 \pm 1.9\,\mu\mathrm{V/K}$ was found at $T = 300$ K,[6] which compares reasonably well to our calculated values of $Q_{\mathrm{M0}}^{\mathrm{NH_2-TT1}} = 10.52\,\mu\mathrm{V/K}$ and $Q_{\mathrm{M0}}^{\mathrm{NH_2-TT2}} = 4.6\,\mu\mathrm{V/K}$ for the same T. Furthermore, recent calculations within a DFT approach with an approximate quasiparticle self-energy correction for comparable geometries showed similar results to ours.[40] For biphenyl-dithiol, the comparison is complicated by the fact that our calculated values vary by two orders of magnitude for the different geometries, i.e., $Q_{\mathrm{M0}}^{\mathrm{S-HH}} = 0.11\,\mu\mathrm{V/K}$, $Q_{\mathrm{M0}}^{\mathrm{S-BB}} = 39.14\,\mu\mathrm{V/K}$, $Q_{\mathrm{M0}}^{\mathrm{S-TT}} = 28.08\,\mu\mathrm{V/K}$ at $T = 300$ K. They scatter indeed around the experimental result of $Q_{\mathrm{M0}}^{\mathrm{S-EXPT}} = 12.9 \pm 2.2\,\mu\mathrm{V/K}$.[4] To our knowledge, the thermopower of cyano-terminated biphenyls has not yet been reported. A trend by the DFT calculations to overestimate the thermopower can nevertheless be recognized.[40] It is expected from the typical overestimation of experimental conductance values,[28] attributed mostly to the interpretation of Kohn-Sham eigenvalues as approximate quasiparticle energies.[41,42] According to Eqs. (8) and (9), an underestimation of $|\tilde{\varepsilon}|$ leads to an overestimation of $|Q|$. However, finite-temperature effects due to fluctuations of the geometries and the electron-vibration interaction, not accounted for in our calculations, may also play a role in the room-temperature experiments.

The transport through the well-conjugated molecules M0-M4 is dominated by the π electrons, and we have shown in Refs. 18, 19, and 28 that for these molecules the conductance arises from one transmission eigenchannel of π character.[19,28] Hence, we would expect their thermopower to follow Eq. (3).

TABLE I. Torsion angle φ in units of degrees and the thermopower Q at $T = 10$ K in units of μV/K for all junction geometries.

	S-HH		S-BB		S-TT1		NH_2-TT1		NH_2-TT2		CN-TT1		CN-TT2	
	φ	Q	φ	Q	φ	Q	φ	Q	φ	Q	φ	Q	φ	Q
M0	35.1	0.002	12.9	1.140	17.9	0.907	32.9	0.343	33.2	0.150	33.1	−2.389	35.3	−1.566
M1	0.3	0.064	0.1	1.313	0.4	1.280	0.2	0.436	0.7	0.201	0.7	−2.281	0.1	−1.423
M2	19.8	0.048	19.3	1.208	17.2	1.266	20.4	0.429	19.1	0.191	19.5	−2.252	20.2	−1.404
M3	42.3	0.032	42.1	1.127	42.0	1.200	46.3	0.382	46.3	0.189	45.1	−1.878	46.4	−1.158
M4	60.7	0.034	53.0	1.006	60.8	0.981	61.6	0.400	58.4	0.158	59.2	−1.657	59.9	−0.938
M7	89.6	0.019	84.0	0.298	83.4	0.981	87.4	0.191	87.3	0.091	89.6	−1.173	89.9	−0.632

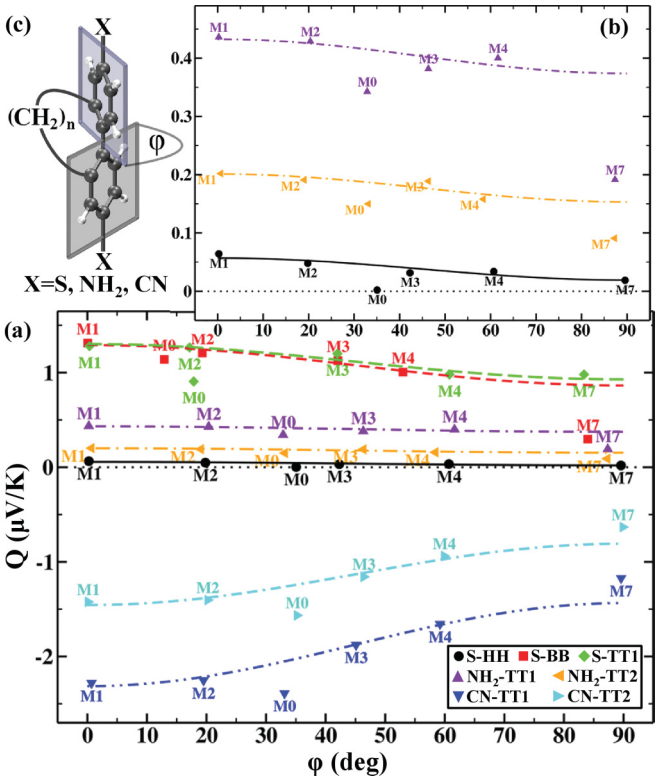

FIG. 3. (Color online) (a) Evolution of Q with increasing φ for all contact geometries. The symbols represent the thermopower values calculated with DFT at $T = 10$ K, and the lines are obtained by fitting Eq. (3) to M1-M4 for each type of junction. (b) Zoom in on the Q values for S-HH, NH_2-TT1, and NH_2-TT2. (c) Schematic of the studied biphenyl derivatives and definition of the torsion angle φ.

Despite the variations of Q with anchoring groups and binding positions, we find a weak $\cos^2\varphi$-like decrease of the absolute values for M1-M4 for all types of geometries. M0, however, deviates from this trend. Although the electron-donating effect of the alkyl chains is expected to be small, it increases Q for M1-M4 as compared to M0. To clarify this, we calculated by means of electrostatic potential fitting and a Löwdin population analysis the charge transferred from the alkyl side chains to the two phenyl rings for the hydrogen-terminated ($X = H$ in Fig. 1), isolated gas-phase molecules. Both methods yield an overall negative charge on the phenyl rings which is practically independent of the alkyl chain length. Therefore, the substituent-related energy shift of frontier orbital levels is similar for M1-M4, and the $a + b\cos^2\varphi$ dependence is observed.

Focusing on the thermopower of M1-M4, we extract a and b by fitting their Q with Eq. (3). The precise values are given in Table II, and the corresponding fits are shown as continuous lines in Fig. 3. Additionally, we list in Table II the ratio $r = |Q_{M1} - Q_{M4}|/(Q_{M1} + Q_{M4})$, quantifying the maximal relative decrease of $|Q|$ in that subset of molecules. We find it to vary between 4% and 31%. In detail, we observe the largest relative change for S-HH followed by CN-TT2. CN-TT1, S-BB, S-TT1, and NH_2-TT2 all show a similar r, while it is smallest for NH_2-TT1.

Using the 2LM in the off-resonant transport case and assuming $\tilde{t}^2 \ll \tilde{\varepsilon}^2$ (see also Table III, discussed below), the

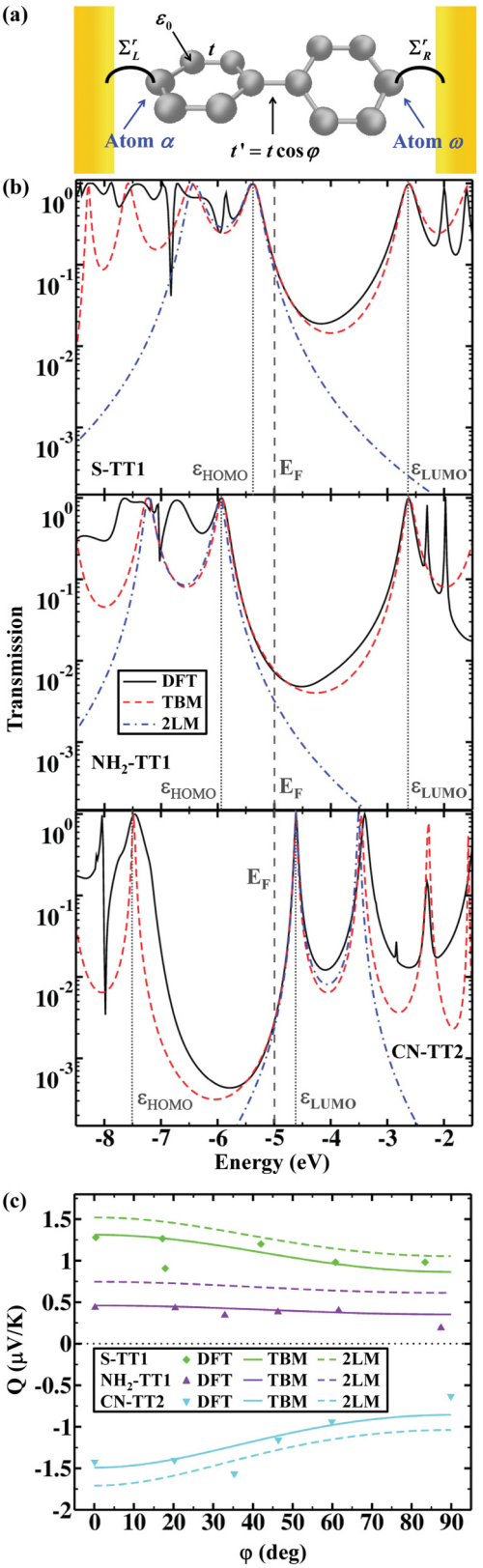

FIG. 4. (Color online) (a) Schematic of the TBM used to fit DFT-based transmission curves. (b) Transmission of M2 as a function of energy calculated with DFT, and the fits using the TBM and the 2LM. (c) Q as a function of φ, comparing values obtained with the TBM and the 2LM to the DFT-based results. In panels (b) and (c), S-TT1, NH_2-TT1, and CN-TT2 junction geometries were selected.

TABLE II. Parameters a and b of Eq. (3) used in Fig. 3 to fit the DFT results of M1-M4 for each type of junction, and the relative change r of Q between M1 and M4.

	a (μV/K)	b (μV/K)	r (%)
S-HH	0.02	0.04	31
S-BB	0.86	0.43	13
S-TT1	0.93	0.37	13
NH_2-TT1	0.37	0.06	4
NH_2-TT2	0.15	0.05	12
CN-TT1	−1.44	−0.89	16
CN-TT2	−0.81	−0.65	20

ratio r can be expressed as $r \approx (1 - \cos^2 \varphi_{M4})\tilde{t}^2/(2\tilde{\varepsilon}^2)$. Here, $\varphi_{M4} \approx 60^\circ$ is the torsion angle of molecule M4, and we have set $\varphi_{M1} = 0$ (see Table I). If the frontier orbitals were more distant from the Fermi energy of the electrodes than determined in our DFT-based charge-transport calculations,[41,42] then the 2LM expression predicts that r should be lower.

For M7, Eq. (3) is not expected to hold because the transport at $\varphi \simeq 90^\circ$ is not π like but proceeds through transmission eigenchannels of π-σ character.[13,28] Furthermore, M7 shows the largest substituent-related shifting effect on the biphenyl backbone in our family of molecules due to the electron-donating nature of the four attached methyl side groups.[13,38,43] Its thermopower hence arises from a detailed interplay between the substituent-related shifting and the large torsion angle, as explained in Ref. 13. We find that the absolute values of Q for M7 are generally lower than predicted by the fits with Eq. (3). Only for S-TT1 and NH_2-TT2 the thermopower seems to follow the $a + b\cos^2\varphi$ dependence, but this is likely coincidental.

C. Transport analysis using the π-orbital tight-binding model and the two-level model

In order to better understand the differences in the thermopower for the various anchoring groups and binding positions, we need to examine the parameters $\tilde{\varepsilon}$, $\tilde{t}$, $\tilde{\Gamma}$ of the 2LM which determine the thermopower according to Eqs. (8) and (9). We note that the dominant, angle-independent term a is a function of $\tilde{\varepsilon}, \tilde{\Gamma}$ only. Thus, to discuss main anchor-group- and binding-site-related variations of Q for the seven different junction types of Fig. 2, it is sufficient to concentrate on these two parameters. The φ dependence of Q, however, results from the interference of the hybridizing pair of phenyl-ring frontier orbital levels, and b hence depends also on $\tilde{t}$.

We obtain the parameters of the 2LM from the TBM introduced in Ref. 35. The TBM is sketched in Fig. 4(a). Similar to the 2LM, the Hückel-type TBM is characterized by three parameters which are the onsite energy ε_0 of each carbon atom, the nearest-neighbor hopping t between atoms on each of the phenyl rings, and the electrode-related broadening Γ. The inter-ring hopping is given as $t' = t\cos\varphi$. Using the wide-band approximation, we assume all components of the lead self-energy matrices to vanish except for $(\Sigma_L^r)_{\alpha\alpha} = (\Sigma_R^r)_{\omega\omega} = -i\Gamma/2$, with α and ω indicating the terminal carbon atoms of the biphenyl molecule as shown in Fig. 4(a).

TABLE III. Parameters of the TBM ε_0, t, Γ obtained by fitting the DFT-based transmission curves for M1-M4 for each type of junction. The parameters $\tilde{\varepsilon}, \tilde{t}, \tilde{\Gamma}$ of the 2LM are derived from those of the TBM as described in the text. All values are given in units of eV.

	ε_0	t	Γ	$\tilde{\varepsilon}$	$\tilde{t}$	$\tilde{\Gamma}$
S-HH	−4.40	−2.30	0.70	−1.70	−0.68	0.22
S-BB	−4.02	−1.95	1.10	−0.97	−0.58	0.35
S-TT1	−4.00	−1.90	0.96	−0.90	−0.56	0.31
NH_2-TT1	−4.30	−2.29	0.60	−1.59	−0.68	0.19
NH_2-TT2	−4.40	−2.32	0.66	−1.72	−0.69	0.21
CN-TT1	−6.10	−2.00	0.14	0.90	−0.59	0.04
CN-TT2	−6.05	−1.99	0.15	0.94	−0.59	0.05

The parameters ε_0, t, Γ of the TBM are extracted by fitting $\tau(E)$ curves calculated with DFT. We focus on the molecules M1-M4 and set φ to the torsion angle realized in the specific junction geometry (see Table I). Concentrating particularly on the HOMO-LUMO gap and frontier orbital peaks, we find that the fitted TBM generally reproduces well the transmission in that range and that the parameters extracted for M1-M4 are very similar in each of the seven types of junctions. Finally, the parameters of the 2LM are derived from those of the TBM. $\tilde{\varepsilon}$ and $\tilde{t}$ are obtained by evaluating appropriate eigenvalues of the angle-dependent Hückel-type Hamiltonian of the TBM. For $\tilde{\Gamma}$, we identify imaginary parts of complex eigenvalues of the non-Hermitian matrices $(H + \Sigma_L^r + \Sigma_R^r)_{jk}$ for the TBM and the 2LM, respectively.[28] Here, H_{jk} and $(\Sigma_L^r)_{jk}$,$(\Sigma_R^r)_{jk}$ represent the matrix elements of the Hamiltonian and of the electrode self-energies in the corresponding model. All the parameters determined in this way are listed in Table III. For M2, transmission curves calculated with the DFT, the TBM, and the 2LM are shown in Fig. 4(b) for each of the three anchoring groups.

Using the parameters of Table III, we compare in Fig. 4(c) Q as a function of φ for the TBM and 2LM fits with the DFT results. We find that the TBM agrees well with the DFT-based values for the illustrated junction geometries S-TT1, NH_2-TT1, and CN-TT2. The 2LM, instead, overestimates $|Q|$ somewhat. Considering Eq. (2) and the transmission curves in Fig. 4(b), we attribute this to an underestimation of $\tau(E_F)$ and an overestimation of $|\partial_E\tau(E_F)|$. All results exhibit a consistent weak dependence of Q on φ.

The data in Table III show that transport through the biphenyl molecules is off resonant with the relation $\tilde{\Gamma} \ll |\tilde{\varepsilon}|$ being well fulfilled. As argued in Sec. III A, a,b should thus take the same sign and change it together with Q when the transport for S- and NH_2-linked molecules changes from HOMO to LUMO dominated for CN anchors. This is consistent with our findings in Figs. 3 and 4(c), and explains the decrease of $|Q|$ with increasing φ.

Since Eq. (3) is based on the low-temperature expansion of Q as given by Eq. (2), there could be modifications to the $a + b\cos^2\varphi$ law when the full energy dependence of $\tau(E)$ is taken into account at finite temperatures via Eq. (1). However, the transmissions of the biphenyl molecules are relatively smooth around E_F [see Fig. 4(b)]. For this reason, we find that the linear temperature dependence of Q in Eq. (2) remains a good approximation up to room temperature,

leaving the $a + b\cos^2\varphi$ dependence unaffected. While we do not show here the behavior of the thermopower at different T, we demonstrated the decrease of $|Q|$ with φ at $T =$ 298 K in Ref. 13 for the twisted biphenyl molecule, applying Eq. (1). Figure 2(a) of Ref. 22 shows that transport is strongly off resonant also in the work of Finch *et al*. and that the HOMO dominates the transmission. This is consistent with our findings in Fig. 4(b). The 2LM should hence apply in Ref. 22, and the positive Q should decrease with φ in their Fig. 3(b) in the whole temperature range between 0 and 300 K. Instead, they report an increase of Q with φ. The methodologies applied here and in Ref. 22 are similar, but differ in the details. With our cluster-based approach,[29] relying on the DFT implementation in TURBOMOLE,[23] we genuinely describe a single-molecule contact, while the SIESTA-based approach of Finch *et al*. considers a two-dimensional array of parallel molecular junctions. We can only speculate about the origin of the puzzling results in Ref. 22. They could range from a trivial confusion of planar and perpendicular ring orientations of the biphenyl molecule to a numerical problem in their determination of the thermopower or a parasitic interaction effect between the neighboring biphenyl molecules.

Coming back to our discussion of the differences of the thermopower for the various anchoring groups and binding positions in Fig. 3, we observe that $\tilde{\varepsilon}$ is around 0.6 to 0.8 eV closer to E_F for S-BB and S-TT1 as compared to S-HH, NH_2-TT1, and NH_2-TT2, which explains their larger Q. For the CN-terminated molecules, $|\tilde{\varepsilon}|$ is comparable to those for S-BB and S-TT1. Slightly larger values of $|Q|$ for CN result from the very small broadenings $\tilde{\Gamma}$. Furthermore, for both NH_2 and CN, $\tilde{t}$ and $\tilde{\Gamma}$ are essentially independent of the binding position, and the difference in Q between TT1 and TT2 hence stems from the changes in the alignment of the HOMO and LUMO levels.

IV. CONCLUSIONS

We have analyzed theoretically the thermopower of single-molecule junctions consisting of biphenyl derivatives contacted to gold electrodes. Our DFT-based study with the three anchors S, NH_2, and CN shows a positive thermopower for S or NH_2 and a negative one for CN. For the junction geometries considered, different binding sites did not affect the sign of Q but led to variations in absolute value. For thiolated molecules in bridge and top binding sites, Q can be up to two orders of magnitude larger than for molecules bonded in hollow position. In contrast, the variations for the two considered top binding sites were around a factor of 2 for NH_2 and CN anchors. We have explained these observations by the changes in the level alignment of current-carrying frontier molecular orbitals. They are caused by the binding-site-dependent charge transfer at the metal-molecule interface.

The main purpose of this work was the study of the dependence of the thermopower on conjugation for an experimentally relevant system. In our set of six biphenyl derivatives, the conjugation was controlled by the torsion angle φ between the phenyl ring planes, and it was varied stepwise between 0° and 90° by means of alkyl side chains attached to the molecules. Despite the sensitivity of the thermopower to the precise geometry at the molecule-metal interface, we observed for all investigated types of junction configurations a decrease in $|Q|$ with increasing φ, following a characteristic $a + b\cos^2\varphi$ law. We explained this behavior in terms of a two-level model, which considers the pair of hybridizing frontier orbitals on the phenyl rings. Predictions by this model of a simultaneous change in sign of Q,a,b for a change from HOMO- to LUMO-dominated transport in the off-resonant situation are consistent with our DFT results. Overall, the influence of conjugation on the thermopower is much less pronounced than on the conductance.

We propose to measure the $a + b\cos^2\varphi$ dependence of the thermopower for the set of biphenyl molecules studied here. Using alkyl chains of different lengths, parasitic substituent-related shifts in Q, superimposed on the weak $a + b\cos^2\varphi$ dependence, are largely avoided. Depending on binding site and employed anchoring group, relative variations of Q of around 15% are expected between M1 and M4. Since frontier molecular orbital energies are likely positioned closer to E_F in our calculations than in the experiment, the relative changes of Q with φ are expected to be somewhat smaller than in our theoretical predictions. Nevertheless, we suggest that the variations of the thermopower with torsion angle are experimentally detectable.

ACKNOWLEDGMENTS

We acknowledge fruitful discussions with A. Bagrets, F. Evers, and V. Meded, and thank the TURBOMOLE GmbH for providing us with the TURBOMOLE source code. M.B. and G.S. were supported through the DFG Center for Functional Nanostructures (Project C3.6), the DFG priority program 1243, and the Initial Training Network "NanoCTM" (Grant No. FP7-PEOPLE-ITN-2008-234970), F.P. through the Young Investigator Group, L.A.Z. by the EU through the BIMORE Network (MRTN-CT-2006-035859) and by the Comunidad de Madrid through the program NANOBIOMAGNET (S2009/MAT1726), and J.K.V. through the Academy of Finland. D.V. and M.M. acknowledge funding by the Swiss National Science Foundation and the Swiss National Center of Competence in Research "Nanoscale Science." The work of A.M. and T.W. was financed by the Swiss National Science Foundation (200021.124643, NFP62), the Initial Training Network FUNMOLS, the DFG priority program 1243, and the University of Bern.

*marius.buerkle@kit.edu

[1] C. J. Vineis, A. Shakouri, A. Majumdar, and M. G. Kanatzidis, Adv. Mater. **22**, 3970 (2010).

[2] Y. Dubi and M. Di Ventra, Rev. Mod. Phys. **83**, 131 (2011).

[3] J. A. Malen, S. K. Yee, A. Majumdar, and R. A. Segalman, Chem. Phys. Lett. **491**, 109 (2010).

[4]P. Reddy, S.-Y. Jang, R. A. Segalman, and A. Majumdar, Science **315**, 1568 (2007).
[5]B. Ludoph and J. M. van Ruitenbeek, Phys. Rev. B **59**, 12290 (1999).
[6]J. A. Malen, P. Doak, K. Baheti, T. D. Tilley, R. A. Segalman, and A. Majumdar, Nano Lett. **9**, 1164 (2009).
[7]A. Tan, J. Balachandran, S. Sadat, V. Gavini, B. D. Dunietz, S.-Y. Jang, and P. Reddy, J. Am. Chem. Soc. **133**, 8838 (2011).
[8]K. Baheti, J. A. Malen, P. Doak, P. Reddy, S.-Y. Jang, T. D. Tilley, A. Majumdar, and R. A. Segalman, Nano Lett. **8**, 715 (2008).
[9]J. R. Widawsky, P. Darancet, J. B. Neaton, and L. Venkataraman, Nano Lett. **12**, 354 (2011).
[10]S. K. Yee, J. A. Malen, A. Majumdar, and R. A. Segalman, Nano Lett. **11**, 4089 (2011).
[11]M. Paulsson and S. Datta, Phys. Rev. B **67**, 241403 (2003).
[12]F. Pauly, J. K. Viljas, M. Bürkle, M. Dreher, P. Nielaba, and J. C. Cuevas, Phys. Rev. B **84**, 195420 (2011).
[13]F. Pauly, J. K. Viljas, and J. C. Cuevas, Phys. Rev. B **78**, 035315 (2008).
[14]S.-H. Ke, W. Yang, S. Curtarolo, and H. U. Baranger, Nano Lett. **9**, 1011 (2009).
[15]M. Galperin, A. Nitzan, and M. A. Ratner, Mol. Phys. **106**, 397 (2008).
[16]N. Sergueev, S. Shin, M. Kaviany, and B. Dunietz, Phys. Rev. B **83**, 195415 (2011).
[17]L. Venkataraman, J. E. Klare, C. Nuckolls, M. S. Hybertsen, and M. L. Steigerwald, Nature (London) **442**, 904 (2006).
[18]A. Mishchenko, D. Vonlanthen, V. Meded, M. Bürkle, C. Li, I. V. Pobelov, A. Bagrets, J. K. Viljas, F. Pauly, F. Evers, M. Mayor, and T. Wandlowski, Nano Lett. **10**, 156 (2010).
[19]A. Mishchenko, L. A. Zotti, D. Vonlanthen, M. Bürkle, F. Pauly, J. C. Cuevas, M. Mayor, and T. Wandlowski, J. Am. Chem. Soc. **133**, 184 (2011).
[20]D. Vonlanthen, A. Mishchenko, M. Elbing, M. Neuburger, T. Wandlowski, and M. Mayor, Angew. Chem., Int. Ed. **48**, 8886 (2009).
[21]J. Rotzler, D. Vonlanthen, A. Barsella, A. Boeglin, A. Fort, and M. Mayor, Eur. J. Org. Chem. **2010**, 1096 (2010).
[22]C. M. Finch, V. M. García-Suárez, and C. J. Lambert, Phys. Rev. B **79**, 033405 (2009).
[23]R. Ahlrichs, M. Bär, M. Häser, H. Horn, and C. Kölmel, Chem. Phys. Lett. **162**, 165 (1989).
[24]J. P. Perdew, Phys. Rev. B **33**, 8822 (1986).
[25]A. D. Becke, Phys. Rev. A **38**, 3098 (1988).
[26]F. Weigend and R. Ahlrichs, Phys. Chem. Chem. Phys. **7**, 3297 (2005).
[27]D. Andrae, U. Häußermann, M. Dolg, H. Stoll, and H. Preuß, Theor. Chim. Acta **77**, 123 (1990).
[28]M. Bürkle, J. K. Viljas, D. Vonlanthen, A. Mishchenko, G. Schön, M. Mayor, T. Wandlowski, and F. Pauly, Phys. Rev. B **85**, 075417 (2012).
[29]F. Pauly, J. K. Viljas, U. Huniar, M. Häfner, S. Wohlthat, M. Bürkle, J. C. Cuevas, and G. Schön, New J. Phys. **10**, 125019 (2008).
[30]H. van Houten, L. W. Molenkamp, C. W. J. Beenakker, and C. T. Foxon, Semicond. Sci. Technol. **7**, B215 (1992).
[31]Y.-S. Liu and Y.-C. Chen, Phys. Rev. B **79**, 193101 (2009).
[32]J. Fransson and M. Galperin, Phys. Chem. Chem. Phys. **13**, 14350 (2011).
[33]F. Pauly, J. K. Viljas, J. C. Cuevas, and G. Schön, Phys. Rev. B **77**, 155312 (2008).
[34]J. M. Ziman, *Electrons and Phonons* (Oxford University Press, Oxford, UK, 2001).
[35]J. K. Viljas, F. Pauly, and J. C. Cuevas, Phys. Rev. B **77**, 155119 (2008).
[36]M. Yu, N. Bovet, C. J. Satterley, S. Bengió, K. R. J. Lovelock, P. K. Milligan, R. G. Jones, D. P. Woodruff, and V. Dhanak, Phys. Rev. Lett. **97**, 166102 (2006).
[37]L. Venkataraman, J. E. Klare, I. W. Tam, C. Nuckolls, M. S. Hybertsen, and M. L. Steigerwald, Nano Lett. **6**, 458 (2006).
[38]C. Hansch, A. Leo, and R. W. Taft, Chem. Rev. **91**, 165 (1991).
[39]L. A. Zotti, T. Kirchner, J.-C. Cuevas, F. Pauly, T. Huhn, E. Scheer, and A. Erbe, Small **6**, 1529 (2010).
[40]S. Y. Quek, H. J. Choi, S. G. Louie, and J. B. Neaton, ACS Nano **5**, 551 (2011).
[41]S. Y. Quek, L. Venkataraman, H. J. Choi, S. G. Louie, M. S. Hybertsen, and J. B. Neaton, Nano Lett. **7**, 3477 (2007).
[42]M. Strange, C. Rostgaard, H. Häkkinen, and K. S. Thygesen, Phys. Rev. B **83**, 115108 (2011).
[43]C. H. Suresh and S. R. Gadre, J. Am. Chem. Soc. **120**, 7049 (1998).